On the Power and Beam Dependency of Load Modulation in mmWave Active Antenna Arrays

Alberto Brihuega[1], Matias Turunen[1], Lauri Anttila[1], Thomas Eriksson[2], Mikko Valkama[1]
[1]Tampere University, Department of Electrical Engineering, Tampere, Finland
[2]Chalmers University of Technology, Department of Electrical Engineering, Gothenburg, Sweden
alberto.brihuegagarcia@tuni.fi

***Abstract*— Linearization of active antenna arrays is gaining increasing interest due to their wide applicability in 5G New Radio (NR) networks. As direct access to the output ports of the power amplifiers (PAs) in highly integrated millimeter-wave (mmW) active arrays is difficult, different over-the-air (OTA) digital predistortion (DPD) solutions have been recently proposed. Large majority of such solutions build on the assumption that the nonlinear behaviors of the parallel PA units are independent of the beam direction. However, in this paper, we show through comprehensive OTA measurements on a commercial 64-element active array operating at 28 GHz, that the nonlinear distortion characteristics and the involved load modulation phenomenon largely depend on the beam direction as well as on the considered transmit power, and also that the beam-dependence increases with increasing transmit power. The findings of the measurements are also connected to the state-of-the-art PA models, paving the way towards the development of more efficient DPD solutions and the associated parameter learning methods for mmW active antenna array transmitters.**

***Keywords*— 5G NR, digital predistortion, millimeter-waves, phased arrays, power amplifiers, RF measurements.**

I. Introduction

The base station (BS) units of the emerging 5G New Radio (NR) networks will deploy dozens or even hundreds of antenna and power amplifier (PA) units, particularly at the so-called frequency range 2 (FR2) referring to the operating bands within 24-40 GHz [1]. Therefore, in order to allow for reasonable form factors, bulky isolators between PAs and antennas, commonly deployed in legacy systems, are avoided, allowing thus for a very compact integration of the PAs and antennas in the same shielding [2]. As a consequence, however, the mutual coupling among the different antennas is considerably higher and can drive the output ports of the PAs. This results in an apparent load variation, commonly referred to as load modulation [2], [3], impacting also the operating conditions and thus the nonlinear behavior of the PAs. Accordingly, the so-called dual-input behavioral models have been recently proposed [3], to model PAs driven by signals at both their input and output ports, and are widely adopted in the current state-of-the-art [2]–[5].

In highly integrated mmW array transmitters, having access to the signals at the output ports of the PAs is no longer necessarily feasible. Hence, the development of over-the-air (OTA) learning based DPD solutions is drawing a lot of interest currently, see, e.g., [2], [4]–[8]. In such methods, a test receiver located in the far field is adopted, which measures the combined OTA signal, and provides feedback towards the transmitter entity, one way or another, for DPD parameter estimation purposes [4], [6]–[8]. This enables the linearization of the main beam direction, where most of the nonlinear distortion is radiated at [9]. However, in practice, the beam(s) will be steered towards the intended receivers, thus it is not necessarily possible to directly observe the main beam signal. Hence, [6] proposed to reconstruct the main beam signal from consecutive observations of the side lobes for different main beam directions, building on the assumption that the PA characteristics are independent of the beam direction. Similarly, [7] proposes an alternative algorithm to reconstruct the main beam signal while considering that the test receiver antennas are embedded within the actual array transmitter. The potential changes on the operation conditions of the PAs due to load modulation are acknowledged, but later assumed negligible under the hypothesis that some coupling mitigation techniques are applied. Furthermore, [4] proposes a different OTA learning technique through direct measurements of the main beam signal from a far field test receiver, while also accounting for the potential crosstalk taking place in the transmitter, in a manner similar to [3]. However, the potential changes in the transmitter nonlinear characteristics due to the beam-dependent load modulation are not considered. Finally, [8] proposes to compensate for the mutual differences between the PA units in beamforming transmitters through dedicated analog tuning boxes, so that all PAs behave mutually the same way. By doing so, it is possible to linearize not only the main beam direction but more broadly in the angular domain with a single DPD. However, the tuning boxes are considered to be estimated sequentially, and in an offline mode

In this paper, we study, demonstrate and elaborate on the importance of the load modulation phenomenon and its dependency on the transmit power and beamforming direction, with special focus on actual OTA measurements on a commercial active antenna array with 64 radiating elements operating at 28 GHz. We show that the measured nonlinear characteristics of the active array do indeed change considerably, as a function of the deployed transmit beam, resulting in a direct degradation of the DPD performance if no DPD updates are performed. Importantly, we also show that the beam-dependence of the load modulation, and thus the effective nonlinear distortion

characteristics, are also transmit power dependent – an important observation that has not been reported in the existing literature. Specifically, it is shown that the beam-dependence is stronger at high transmit power levels. After tying the findings into the state-of-the-art PA and DPD models, the paper importantly concludes that new OTA DPD learning techniques are needed, potentially even continuous DPD learning, such that beam- and power-dependent load modulation effects can be efficiently tracked and suppressed, particularly when the active array is operating close to saturation for maximum power efficiency.

The rest of the paper is organized as follows. In Section II, the state-of-the-art nonlinear signal model of the active antenna array under antenna crosstalk is shortly reviewed. The conducted OTA RF measurement system and obtained results are then presented and analyzed in detail in Section III. Lastly, Section IV will provide the concluding remarks.

II. Nonlinear Active Array Model

As the state-of-the-art model, we adopt the dual-input behavioral model of [3] where the incident waves at the input and output ports of the ith PA are denoted as $a_{1i}(n)$ and $a_{2i}(n)$, respectively. To this end, $a_{2i}(n)$ can be expressed as a linear combination of the PA output signals $b_{2l}(n)$, written as

$$a_{2i}(n) = \sum_{l=1}^{L} \lambda_{il}(n) \star b_{2l}(n) \tag{1}$$

where $\lambda_{il}(n)$ denotes the impulse response of the coupling channel between antennas i and l. Furthermore, as shown in [3], the ith PA output under the excitation of $a_{1i}(n)$ and $a_{2i}(n)$ is of the form

$$\begin{aligned} b_{2i}(n) = & \sum_{m_1=0}^{M_1} \sum_{p=0}^{(P_1-1)/2} \alpha_{m_1}^{(2p+1)} a_{1i}(n-m_1)|a_{1i}(n-m_1)|^{2p} \\ & + \sum_{m_2=0}^{M_2} \beta_{0,m_2} a_{2i}(n-m_2) \\ & + \sum_{m_3=0}^{M_3} \sum_{m_4=0}^{M_4} \sum_{p=1}^{(P_2-1)/2} \beta_{m_4 m_3}^{2p+1} a_{1i}(n-m_3) \\ & \times |a_{1i}(n-m_4)|^{2p} \\ & + \sum_{m_5=0}^{M_5} \sum_{m_6=0}^{M_6} \sum_{p=1}^{(P_3-1)/2} \zeta_{m_6 m_5}^{2p+1} a_{2i}^{*}(n-m_5) \\ & \times (a_{1i}(n-m_6))^2 |a_{1i}(n-m_6)|^{2(p-1)}, \end{aligned} \tag{2}$$

where it is assumed that the incident wave at the PA output produces small perturbations around the operation point imposed by $a_{1i}(n)$, and hence, only the linear terms of $a_{2i}(n)$ are considered.

Given a phased-array type of beamforming transmitter, the signals $a_{1i}(n)$ are different phase-rotated and potentially also amplitude-scaled versions of the common modulated signal $a_1(n)$, i.e., $a_{1i}(n) = w_i a_1(n)$, where w_i is the corresponding complex-valued beamforming coefficient at antenna branch i. Therefore, it can be shown that (2) can be re-written as [5]

$$\begin{aligned} b_{2i}(n) = & \sum_{m_1=0}^{M_1} \sum_{p=0}^{(P_1-1)/2} \alpha_{m_1}^{(2p+1)} w_i |w_i|^{2p} a_1(n-m_1) \\ & \times |a_1(n-m_1)|^{2p} \\ & + \sum_{m_2=0}^{M_2} \beta_{0,m2} f_i(n-m_2) \star a_1(n-m_2) \\ & + \sum_{m_3=0}^{M_3} \sum_{m_4=0}^{M_4} \sum_{p=1}^{(P_2-1)/2} \beta_{m_4 m_3}^{2p+1} |w_i|^{2p} \\ & \times f_i(n-m_3) \star a_1(n-m_3) |a_1(n-m_4)|^{2p} \\ & + \sum_{m_5=0}^{M_5} \sum_{m_6=0}^{M_6} \sum_{p=1}^{(P_3-1)/2} \zeta_{m_6 m_5}^{2p+1} w_i^2 |w_i|^{p-1} \\ & \times f_i^{*}(n-m_5) \star a_1^{*}(n-m_5) (a_1(n-m_6))^2 \\ & \times |a_1(n-m_6)|^{2(p-1)}, \end{aligned} \tag{3}$$

which is only a function of the transmit signal $a_1(n)$. $f_i(n) = \sum_{l=1}^{L} w_l \lambda_{il}(n) \star \mu_l(n)$, where $\mu_l(n)$ is an impulse response that models the linear distortion.

III. Over-the-Air Measurements

To study and illustrate how the load modulation depends on the transmit power and beam direction, extensive OTA measurements on a commercial 64-element active antenna array operating at 28 GHz are next conducted. The previous state-of-the-art model in (3) is adopted, to generate the basis functions (BFs) for both the array direct model identification as well as for DPD processing, which are both considered in the measurements. The maximum nonlinearity orders P_1, P_2, P_3 and the memory depths $M_1, \ldots, M_6$ in (3) are set to 9 and 4, respectively. The considered test signal is a 5G NR FR2 specifications [1] compliant OFDM waveform with 200 MHz channel bandwidth, i.e., subcarrier spacing is 60 kHz and 3168 out of the 4096 FFT bins are active subcarriers.

A. mmW OTA Measurement Setup

The Keysight M8190A arbitrary waveform generator is utilized to generate the modulated IF signal centered at 3.5 GHz. Then, an N5183B-MXG signal generator running at 24.5 GHz is utilized together with an external mixer to up-convert the signal to the desired carrier frequency of 28 GHz. The RF signal is fed to two cascaded linear driver PAs, feeding the actual Anokiwave AWMF-0129 active antenna array. The signal then propagates over-the-air and is captured by a horn antenna. The RF signal is then down-converted to 3.5 GHz IF and digitized by the Keysight DSOS804A oscilloscope, which also carries out IF to baseband conversion. The received samples are then processed in a host PC running MATLAB, where the actual direct model estimation as well as the DPD processing and parameter learning are performed, with oversampling factor of 5 wrt. the critical sample rate. The measurement setup is shown in Fig. 1.

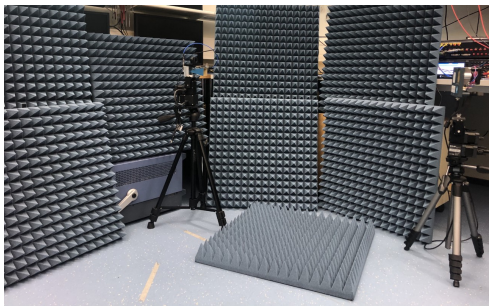

Fig. 1. mmW OTA laboratory measurement setup at 28 GHz.

B. OTA Measurement Results

The measurements are conducted such that the OTA receiver antenna is always kept fixed at a considered location, while the antenna array steers the beam from -40 to 40 degrees with an angular resolution of 5 degrees. For every electrical beam direction, the antenna array is mechanically rotated towards the opposite direction by the same amount, so that the main beam is perfectly aligned with the receiver antenna. The experiments are conducted at three different power levels, which are referred to as low, medium and high power, respectively, so that the potential transmit power effect on the load modulation can be observed. To quantify the load modulation impact, we consider and calculate the adjacent channel error power ratio (ACEPR) and the adjacent channel power ratio (ACPR) [6], [10]. As these are well-known and widely applied metrics in PA direct modeling and DPD research, their exact expressions are omitted, for brevity, while the reader can refer, e.g., to [6], [10].

In Fig. 2, example measured power spectra of the OTA signals corresponding to the high power scenario are depicted for the different considered beam directions. As it can be observed, there are substantial differences in the nonlinear distortion characteristics, which are essentially solely due to the beam-dependent load modulation.

The measured direct model coefficients corresponding to the static nonlinear BFs for the three different EIRP levels are depicted in Fig. 3. The different clouds of points correspond to the instantaneous pth order direct model coefficients of each of the seventeen evaluated beam directions, for $p \in 1, 3, \ldots, 9$. Interestingly, as the transmit power increases and the array approaches saturation, the deviation of the coefficients becomes substantially larger. This reveals that the load modulation becomes more severe at higher transmit power levels, thus demonstrating that the beam-dependence of the load modulation, and thus the effective nonlinear distortion characteristics, are also largely transmit power dependent – an observation which has not been reported in the existing literature.

The larger differences among the different beam directions will result in larger DPD performance and modelling accuracy losses when considering a single set of coefficients to linearize or estimate every beam direction. This is illustrated through Figs. 4 and 5. Specifically, Fig. 4 illustrates how well three different example sets of direct model coefficients, trained at 0, 20 and -20 degrees beam directions, can predict the

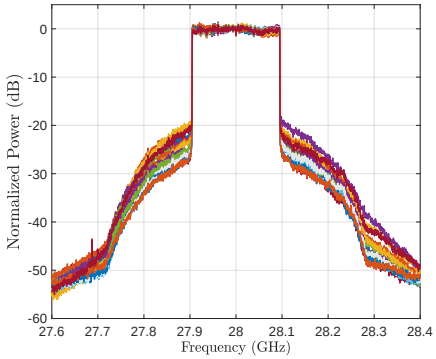

Fig. 2. Spectral snapshots for the 17 different considered beam directions, within -40° to +40°, for the high-power scenario with EIPR $\approx$ +43 dBm.

out-of-band emissions of the OTA received signal across the overall considered range of spatial directions. Naturally, the best modelling accuracy is obtained at the direction for which the models are trained. Then, as the beam is changed, the modelling error increases – a phenomenon that again is more visible at larger effective isotropic radiated power (EIRP) levels. This is in line with the results previously shown in Fig. 3. Similar observations can be made in Fig. 5 when evaluating the DPD linearization performance through the ACPR metric. In this case, two sets of DPD filter coefficients were trained, at 0 and 20 degrees beam directions, utilizing a piece-wise implementation of the dual-input basis-functions and closed-loop gradient-based learning [5]. As can be observed, in the low EIRP scenario, somewhat constant linearization is provided regardless of the beam direction. As the power is increased, the differences in the exact nonlinear characteristics of the antenna array are more pronounced, and the DPD performance clearly degrades when changing the electrical beam direction compared to the one used in DPD learning.

These findings show and infer that future OTA DPD learning solutions need to account for the potential changes in the nonlinear characteristics due to beam-steering, particularly when operating close to array saturation. Such beam- and power-dependence, together with the very wide channel bandwidths in mmW systems, also call for reduced-complexity parameter learning methods that may even be executed continuously.

IV. Conclusions

In this paper, we studied and elaborated on the importance of load modulation on the nonlinear distortion characteristics of highly integrated active antenna arrays through practical OTA experiments, with special focus on mmW 5G NR systems. Specifically, it was shown that the nonlinear distortion characteristics are beam-dependent, and importantly, that the beam-dependence becomes stronger when the transmit power is increased. These findings pave the way towards the development of new DPD techniques and low-complexity DPD learning methods, potentially facilitating even continuous learning, especially in cases when the array is operated close to saturation for maximum power efficiency.

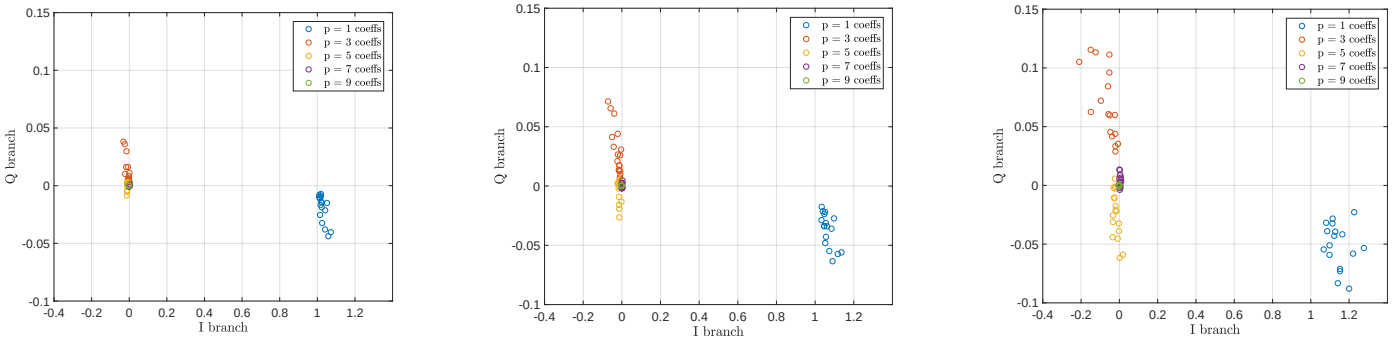

(a) Low-power case, EIRP ≈ +36.5 dBm (b) Medium-power case, EIRP ≈ +39.5 dBm (c) High-power case, EIRP ≈ +43 dBm

Fig. 3. Instantaneous direct model coefficients for different beam directions and power levels. Memory coefficients are omitted for visual simplicity.

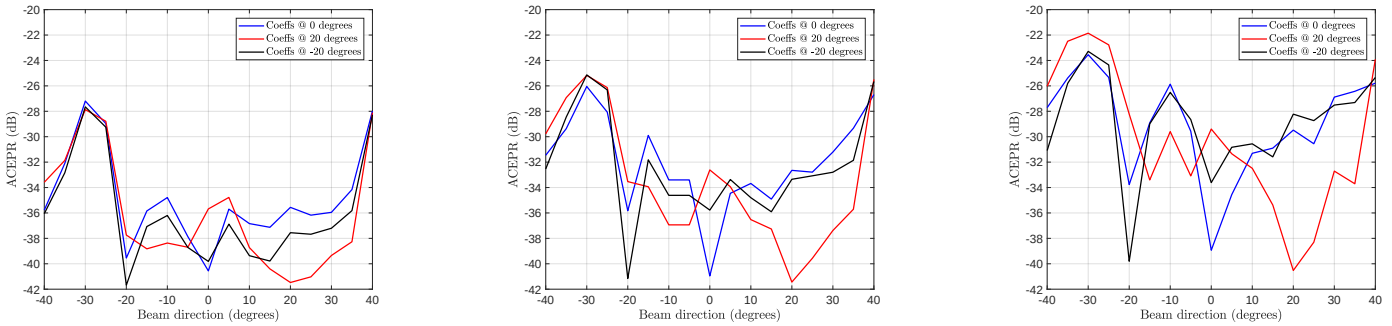

(a) Low-power case, EIRP ≈ +36.5 dBm. (b) Medium-power case, EIRP ≈ +39.5 dBm. (c) High-power case, EIRP ≈ +43 dBm.

Fig. 4. OOB modelling error for three different sets of model coefficients, trained at -20°, 0° and 20°, for three different power levels.

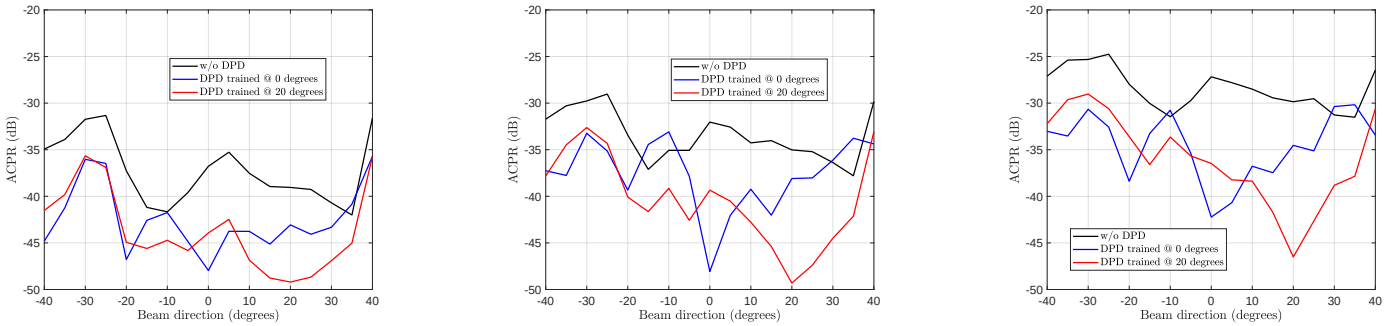

(a) Low-power case, EIRP ≈ +36.5 dBm. (b) Medium-power case, EIRP ≈ +39.5 dBm. (c) High-power case, EIRP ≈ +43 dBm

Fig. 5. Linearization performance for two sets of DPD coefficients, trained at 0° and 20°, as a function of the beam direction and transmit power.

REFERENCES

[1] 3GPP Tech. Spec. 38.104, "NR; Base Station (BS) radio transmission and reception," v15.4.0 (Release 15), Dec. 2018.

[2] C. Fager *et al.*, "Linearity and efficiency in 5G transmitters: New techniques for analyzing efficiency, linearity, and linearization in a 5G active antenna transmitter context," *IEEE Microw. Mag.*, vol. 20, no. 5, pp. 35–49, May 2019.

[3] K. Hausmair *et al.*, "Prediction of nonlinear distortion in wideband active antenna arrays," *IEEE Trans. Microw. Theory Techn.*, vol. 65, no. 11, pp. 4550–4563, Nov 2017.

[4] Q. Luo, X. Zhu, C. Yu, and W. Hong, "Single-receiver over-the-air digital predistortion for massive MIMO transmitters with antenna crosstalk," *IEEE Trans. Microw. Theory Techn.*, pp. 1–15, 2019.

[5] A. Brihuega *et al.*, "Piecewise Digital Predistortion for mmWave Active Antenna Arrays: Algorithms and Measurements," *IEEE Trans. Microw. Theory Techn.*, 2020, Available at: https://arxiv.org/abs/2003.06348.

[6] X. Wang *et al.*, "Digital predistortion of 5G massive MIMO wireless transmitters based on indirect identification of power amplifier behavior with OTA tests," *IEEE Trans. Microw. Theory Techn.*, pp. 1–13, 2019.

[7] X. Liu *et al.*, "Linearization for hybrid beamforming array utilizing embedded over-the-air diversity feedbacks," *IEEE Trans. Microw. Theory Techn.*, pp. 1–14, 2019.

[8] C. Yu *et al.*, "Full-angle digital predistortion of 5G millimeter-wave massive MIMO transmitters," *IEEE Trans. Microw. Theory Techn.*, vol. 67, no. 7, pp. 2847–2860, July 2019.

[9] M. Abdelaziz *et al.*, "Digital Predistortion for Hybrid MIMO Transmitters," *IEEE J. Sel. Topics Signal Process.*, vol. 12, no. 3, June 2018.

[10] A. S. Tehrani *et al.*, "A comparative analysis of the complexity/accuracy tradeoff in power amplifier behavioral models," *IEEE Trans. Microw. Theory Techn.*, vol. 58, no. 6, pp. 1510–1520, June 2010.